Supplemental Figure 1

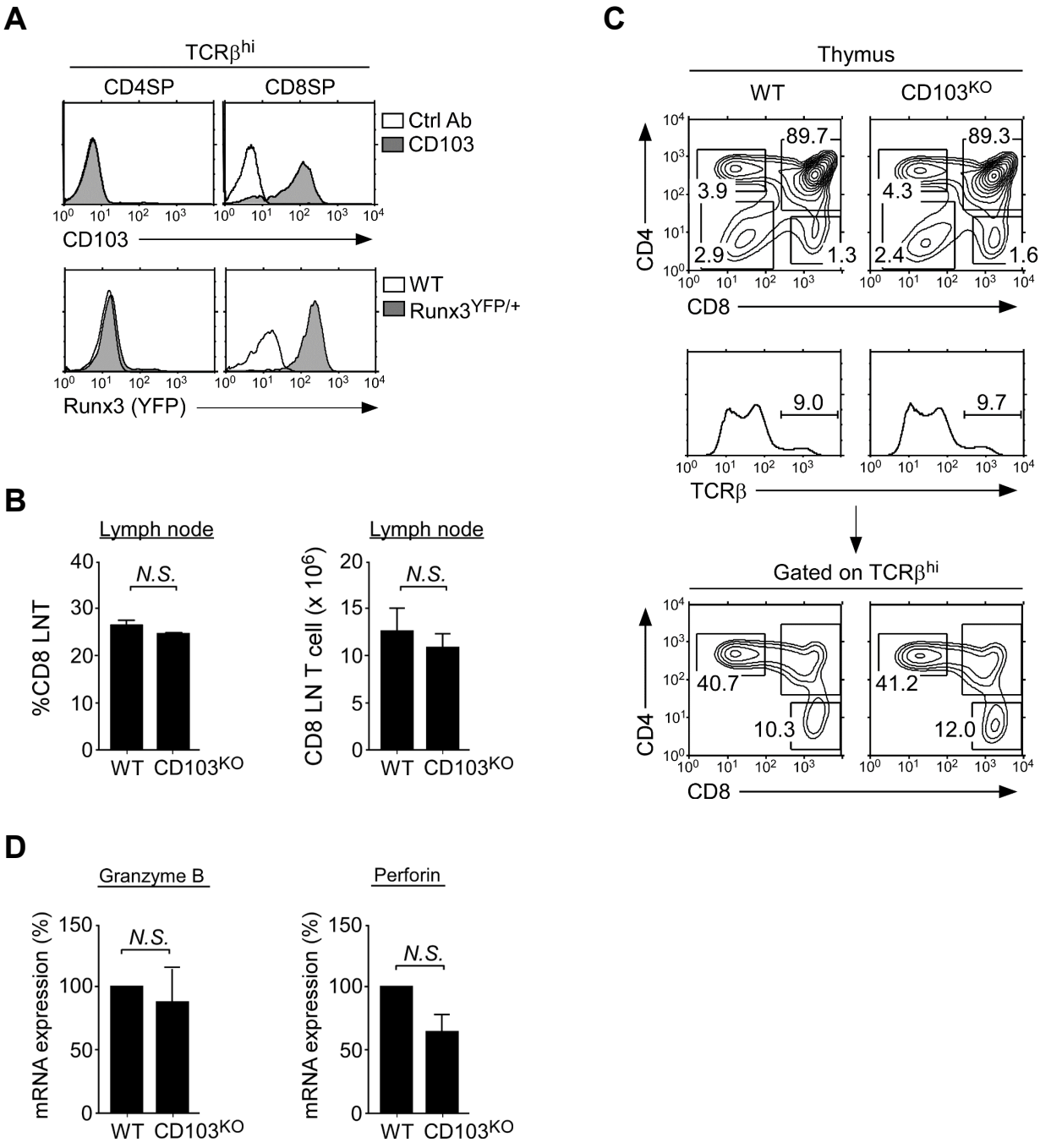

Supplemental Figure 1. Runx3 and CD103 expression on CD8 T cells.
(A) Runx3$^{YFP/+}$ reporter mice were used to determine the expression of CD103 and Runx3 in CD4SP and CD8SP thymocytes. Data are from 5 independent experiments.
(B) Frequency and cell number of TCRβ^{+} CD8 T cells in LN of WT and CD103^{KO} mice. Data are a summary of 8 experiments.
(C) Thymocyte profiles of WT and CD103^{KO} mice. Representative of 8 independent experiments.
(D) Quantitative RT-PCR analysis of Perforin and Granzyme B mRNA in freshly purified WT and CD103^{KO} CD8 LN T cells (relative to β-actin). Data are from 2 independent experiments with a total of 4 WT and CD103^{KO} mice.

Supplemental Figure 2

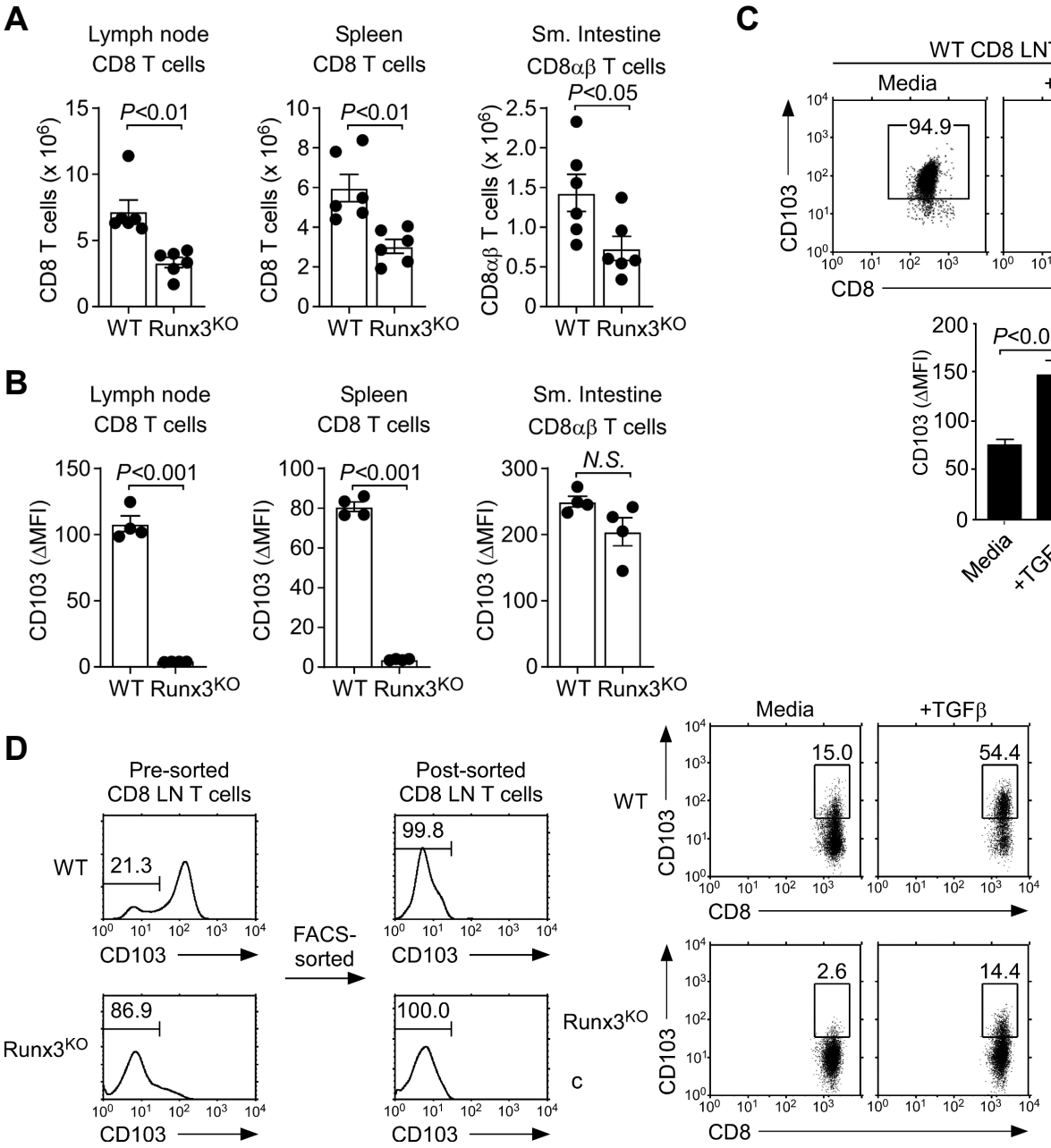

Supplemental Figure 2. T cell differentiation in the absence of Runx3

(A) CD8 T cell numbers in the LN, spleen and small intestine IEL of WT and Runx3^{KO} mice. Data are representative of 3 independent experiments with a total of 6 WT and 6 Runx3^{KO} mice.

(B) Quantification of CD103 expression on WT and Runx3^{KO} CD8 T cells. ΔMFI of CD103 expression was assessed on CD8 T cells of LN, spleen and small intestine IEL of WT and Runx3^{KO} mice. Data are representative of 2 independent experiments with a total of 4 WT and 4 Runx3^{KO} mice.

(C) CD103 surface expression on WT CD8 T cells after 4 days of in vitro stimulation with TGFβ. Mean florescence intensities (MFI) of CD103 expression on the gated CD103^{+} CD8 LN T cells following stimulation. Data are from 2 independent experiments with a total of 6 mice.

(D) Histograms (left) show the purity check for CD103-negative CD8 LN T cells before and after FACS-sorting. Dot plots show CD103 expression on FACS-sorted CD103-negative WT and Runx3^{KO} CD8 LN T cells after 4 days of in vitro stimulation with TGFβ. Data are representative of 3 independent experiments.

Supplemental Figure 3

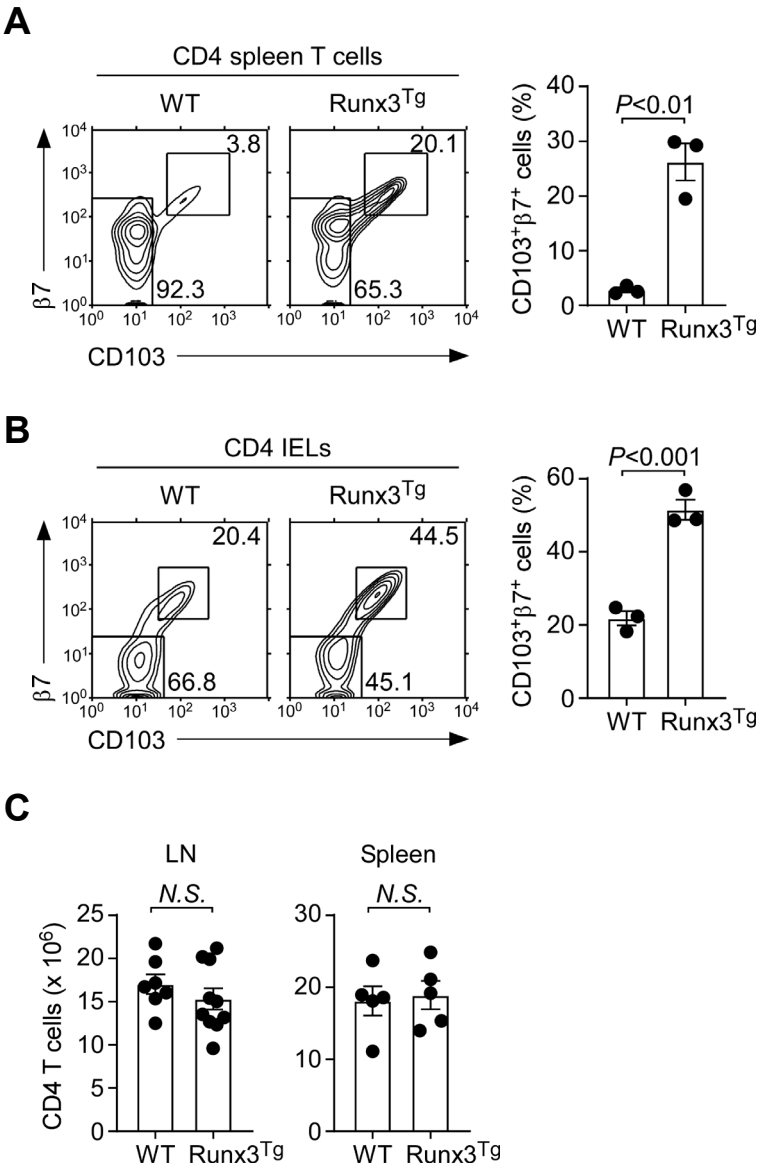

Supplemental Figure 3. Frequencies of CD103$^+$β7$^+$ CD4 T cells in the spleen and IELs of WT and Runx3^{Tg} mice.

Coexpression of CD103 and β7 in CD4 T cells from the spleen (**A**) or small intestine IEL (**B**) of WT and Runx3^{Tg} mice. CD4 T cells were assessed for CD103 and β7, and the frequency of CD103, β7 coexpressing cells were determined. Contour plots are representative, and the bar graphs show the summary of 2 independent experiments with a total of 3 WT and 3 Runx3^{Tg} mice.

(**C**) CD4 T cell numbers in WT and Runx3^{Tg} mice. LN CD4 T cell results are from 7 independent experiments with a total of 7 WT and 10 Runx3^{Tg} mice. Spleen CD4 T cell results are from 5 independent experiments with a total of 5 WT and 5 Runx3^{Tg} mice.

Supplemental Figure 4

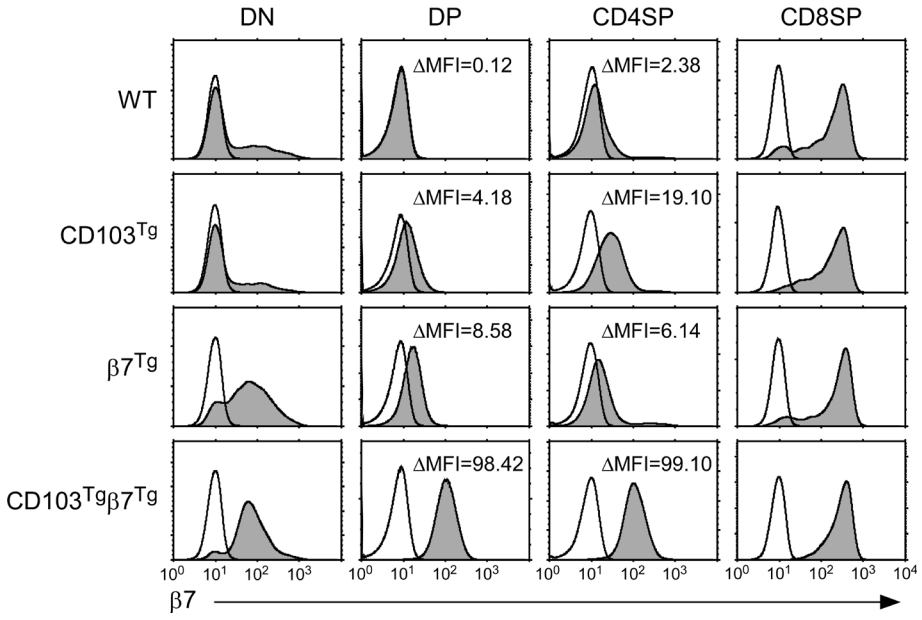

Supplemental Figure 4. Generation of CD103^{+} CD4 T cells by transgenic expression of CD103 and β7

Surface β7 expression on DN, DP, and mature CD4SP and CD8SP thymocytes of WT, CD103^{Tg}, β7^{Tg}, and CD103^{Tg}β7^{Tg} mice. Shaded histograms show anti-β7 staining; open histograms indicate control antibody staining. ΔMean Fluorescence Intensity (ΔMFI) of β7 expression was determined by subtracting the control antibody MFI from CD103 MFI. The results are representative of 7 independent experiments with a total of 7 WT, 7 CD103^{Tg}, 7 β7^{Tg}, and 7 CD103^{Tg}β7^{Tg} mice.

Supplemental Figure 5

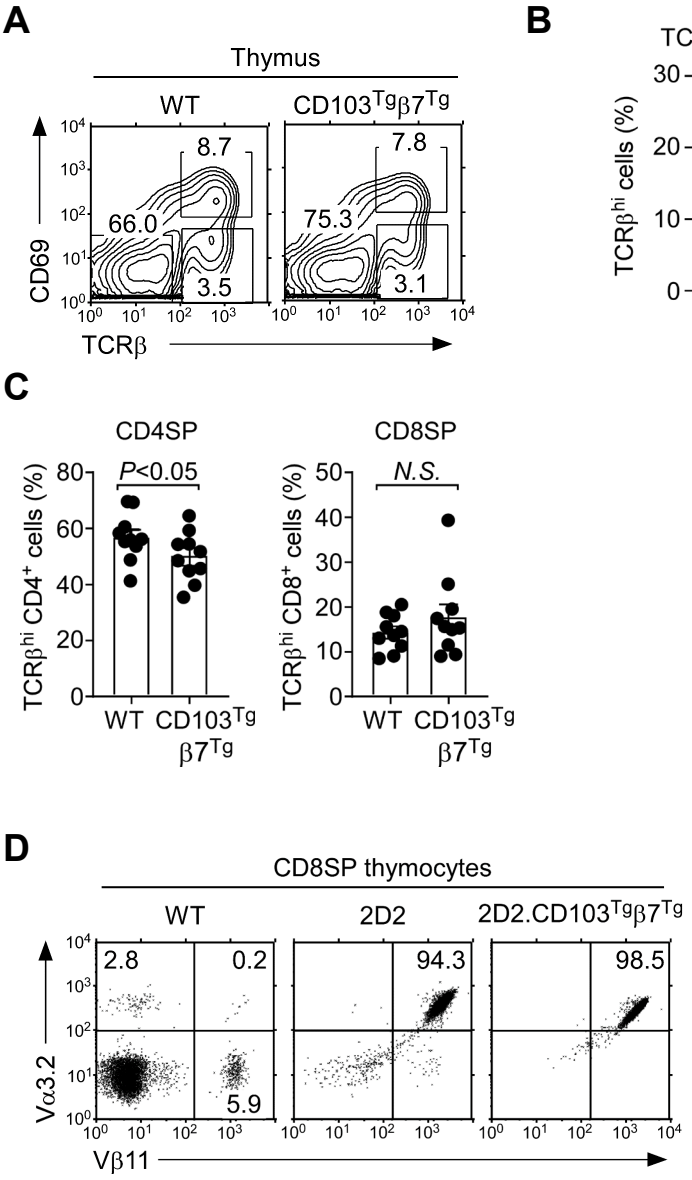

Supplemental Figure 5. Thymocyte differentiation in CD103^{Tg}β7^{Tg} mice

(A) CD69 versus TCRβ thymocyte profiles of WT and CD103^{Tg}β7^{Tg} mice. Data are representative of 2 independent experiments.

(B) Bar graphs show the frequency of TCRβ^{hi} thymocytes in WT and CD103^{Tg}β7^{Tg} mice. Results show the summary of 8 independent experiment with a total of 10 WT and 10 CD103^{Tg}β7^{Tg} mice.

(C) Bar graphs show the frequency of TCRβ^{hi} CD4SP and CD8SP cells among WT and CD103^{Tg}β7^{Tg} thymocytes. The results show the summary of 8 independent experiments with a total of 10 WT and 10 CD103^{Tg}β7^{Tg} mice.

(D) Clonotypic TCR expression in CD8SP thymocytes of 2D2.CD103^{Tg}β7^{Tg} mice. Clonotypic TCR Vβ11 and Vα3.2 expression was assessed on CD8SP cells of WT C57BL/6, 2D2, and 2D2.CD103^{Tg}β7^{Tg} mice.

Supplemental Figure 6

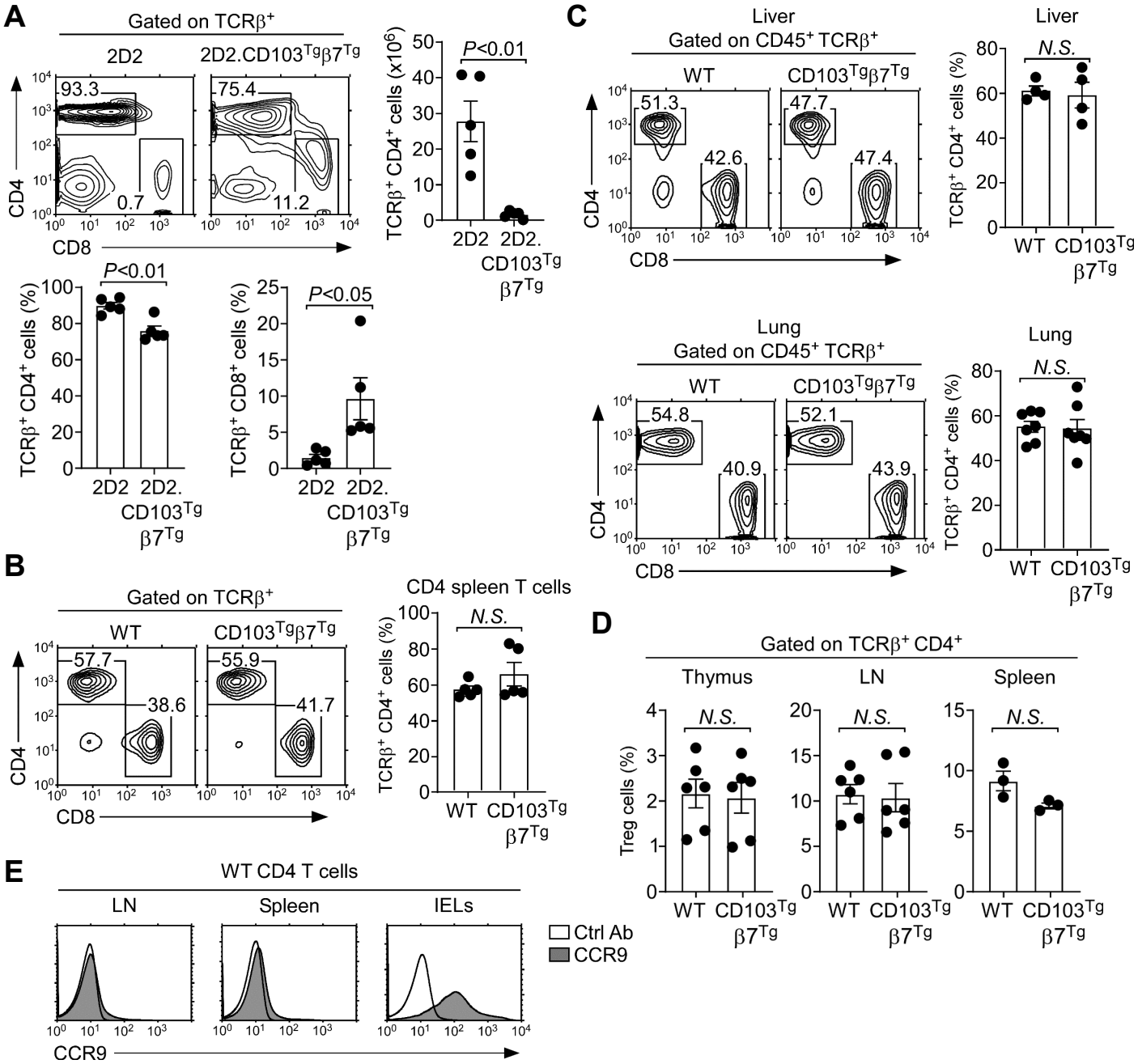

Supplemental Figure 6. CD4 T cells in peripheral organs of CD103^{Tg}β7^{Tg} mice.

(A) CD4 versus CD8 profiles of 2D2 and 2D2.CD103^{Tg}β7^{Tg} thymocytes. Contour plots are representative and bar graph shows summary of 4 independent experiments with total 5 2D2 and 5 2D2.CD103^{Tg}β7^{Tg} mice.

(B) CD4 versus CD8 profiles of splenic T cells of WT and CD103^{Tg}β7^{Tg} mice. Contour plots are representative and bar graph shows summary of 3 independent experiments with total 5 WT and 5 CD103^{Tg}β7^{Tg} mice.

(C) Frequency of CD4 T cells in the liver and lung of WT and CD103^{Tg}β7^{Tg} mice. Data are representative of 3 independent experiments for the liver (top) with 4 WT and 4 CD103^{Tg}β7^{Tg} mice, and 6 independent experiments for the lung (bottom) with total 7 WT and 7 CD103^{Tg}β7^{Tg} mice.

(D) Frequency of CD25^{+}Foxp3^{+} CD4 Treg cells in the thymus, LN and spleen of WT and CD103^{Tg}β7^{Tg} mice. Data show the summary of at least 3 independent experiments.

(E) CCR9 expression on CD4 T cells from LN, spleen and IEL of WT mice.